CFTR as a cAMP-Dependent Regulator of Sodium Channels

M. Jackson Stutts,* Cecilia M. Canessa, John C. Olsen, Maura Hamrick, Jonathan A. Cohn, Bernard C. Rossier, Richard C. Boucher

Cystic fibrosis transmembrane regulator (CFTR), the gene product that is mutated in cystic fibrosis (CF) patients, has a well-recognized function as a cyclic adenosine 3′,5′-monophosphate (cAMP)–regulated chloride channel, but this property does not account for the abnormally high basal rate and cAMP sensitivity of sodium ion absorption in CF airway epithelia. Expression of complementary DNAs for rat epithelial Na^+ channel (rENaC) alone in Madin Darby canine kidney (MDCK) epithelial cells generated large amiloride-sensitive sodium currents that were stimulated by cAMP, whereas coexpression of human CFTR with rENaC generated smaller basal sodium currents that were inhibited by cAMP. Parallel studies that measured regulation of sodium permeability in fibroblasts showed similar results. In CF airway epithelia, the absence of this second function of CFTR as a cAMP-dependent regulator likely accounts for abnormal sodium transport.

Absorption of Na^+ is the dominant basal ion transport process in all adult mammalian species surveyed (*1*). Although airway epithelia can both absorb Na^+ and secrete Cl^-, the means by which they coordinate these opposing processes in switching between basal salt and water absorption and stimulated salt and water secretion has not been explained. CF airway epithelia have an abnormally high rate of Na^+ absorption (*2*)—which reflects an increase in apical membrane Na^+ permeability (*3*, *4*) resulting from Na^+ channels that are overactive, that is, have an increased probability of being open (*5*)—and do not secrete Cl^- in response to cAMP (*1*). We therefore investigated the possible role of CFTR in this coordinate regulation.

Complementary DNAs (cDNAs) encoding the α, β, and γ subunits of rENaC (*6*, *7*) were cotransfected into a clone of MDCK cells (*8*, *9*), a cell line that expresses few functional Na^+ channels and little CFTR (*10*). Proteins corresponding to rENaC subunits (Fig. 1A) and 40 to 60 μA/cm² of resting current (Fig. 1B) (*11*) were observed in rENaC-transfected (MDCK/rENaC) cells that were induced for 24 hours in 1 μM dexamethasone and 2 mM butyrate, whereas neither property was a feature of the parent MDCK cells. The induced current was identified as Na^+ current by the lack of effect of Cl^--free solutions (*12*) (Fig. 1B) and by strong inhibition by amiloride and the amiloride analogs benzamil and phenamil (Fig. 1C, left panel). The induced current was resistant to 5-(*N*-ethyl-*N*-isopropyl)-2′-4′-amiloride (EIPA) (*6*, *7*, *13*). Human airway epithelia expressed homologs of α-, β-, and γ-rENaC (*14*) and exhibited a $Na^+ > K^+$ permselectivity of apical membrane Na^+ conductance (*3*, *4*) that was similar to that of rENaC (*7*), and their Na^+ currents were inhibited by amiloride and its analogs in a pattern that was nearly identical to that of MDCK/rENaC cells (Fig. 1C, right panel).

To test the effect of human CFTR on Na^+ channel function, we exposed MDCK/rENaC cells to an adenoviral vector containing the CFTR cDNA [Ad5-CBC*FTR* (*15*)] to generate large amounts of CFTR protein (Fig. 2, A and B) (*16*). Ad5-CBC*FTR*–infected MDCK/rENaC cells exhibited significantly reduced amiloride-sensitive Na^+ current in a Cl^--free solution compared with that exhibited by control-infected MDCK/rENaC cells (Fig. 2C). These data suggest an inverse relation between CFTR expression and the basal rate of Na^+ absorption.

In our previous study of freshly excised human tissues, Na^+ absorption was abnormally stimulated in CF airway epithelium by isoproterenol or forskolin (*2*). MDCK/rENaC cells that had a high rate of Na^+ absorption but were not transfected with CFTR responded to forskolin with increased amiloride-sensitive Na^+ absorption (Fig. 2D, left panel); this response is similar to that of human CF airway epithelium (*2*). In contrast, MDCK/rENaC cells infected with Ad5-CBC*FTR* responded to forskolin with a slight but significant decrease in the amiloride-sensitive Na^+ current (Fig. 2D, right panel). Thus, expression of CFTR in induced MDCK/rENaC cells reverses the direction of regulation of Na^+ current by forskolin (Fig. 2E).

Transepithelial Na^+ currents result from the series activities of an apical membrane Na^+ permeability (P_{Na^+}) and the basolateral Na^+- and K^+-dependent adenosine triphosphatase (Na^+,K^+-ATPase) pump (*17*). P_{Na^+} is rate-limiting for Na^+ transport in airway epithelia (*3*) and is raised in CF airway epithelia (*4*, *18*). To study regulatory interactions between CFTR and rENaC directly at the level of P_{Na^+}, we expressed

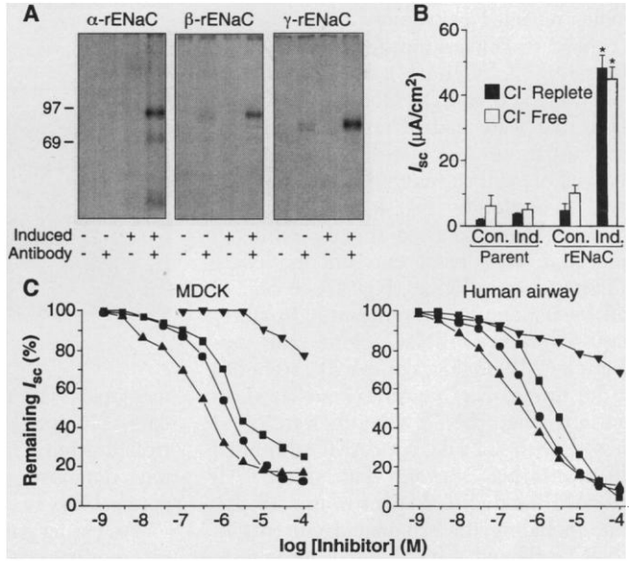

Fig. 1. Induced Na^+ channel function in MDCK cells. (**A**) Expression of rENaC subunits in MDCK cells, as recognized in transfected and induced cells by immunoprecipitation. (**B**) Current (I_{sc}) generated by parent and rENaC-transfected cells, with and without induction, in normal KBR (solid bars) and bilateral Cl^--free KBR (open bars) (n = 6 to 12 in each group). Asterisks denote significant differences between the induced (Ind.) and control (Con.) currents (unpaired t analysis, $P <$ 0.01). (**C**) Pharmacologic characterization of rENaC in MDCK cells and endogenous Na^+ transport in human airway epithelia. Inhibition of Na^+ current by amiloride (■) and the amiloride analogs benzamil (●), phenamil (▲), and EIPA (▼) is shown as a function of inhibitor concentration. Induced MDCK/rENaC cells (left panel) and cultured normal human airway epithelia (right panel) were studied in bilateral Cl^--free KBR. Each symbol represents the mean of three separate experiments.

M. J. Stutts, J. C. Olsen, M. Hamrick, R. C. Boucher, Cystic Fibrosis/Pulmonary Research and Treatment Center, University of North Carolina at Chapel Hill, Chapel Hill, NC 27599–7020, USA.
C. M. Canessa and B. C. Rossier, Institut de Pharmacologie et de Toxicologie, Universite Lausanne, Rue du Bugnon 27, CH-1005 Lausanne, Switzerland.
J. A. Cohn, Duke University and Veterans Administration Medical Centers, Durham, NC 27710, USA.
*To whom correspondence should be addressed.

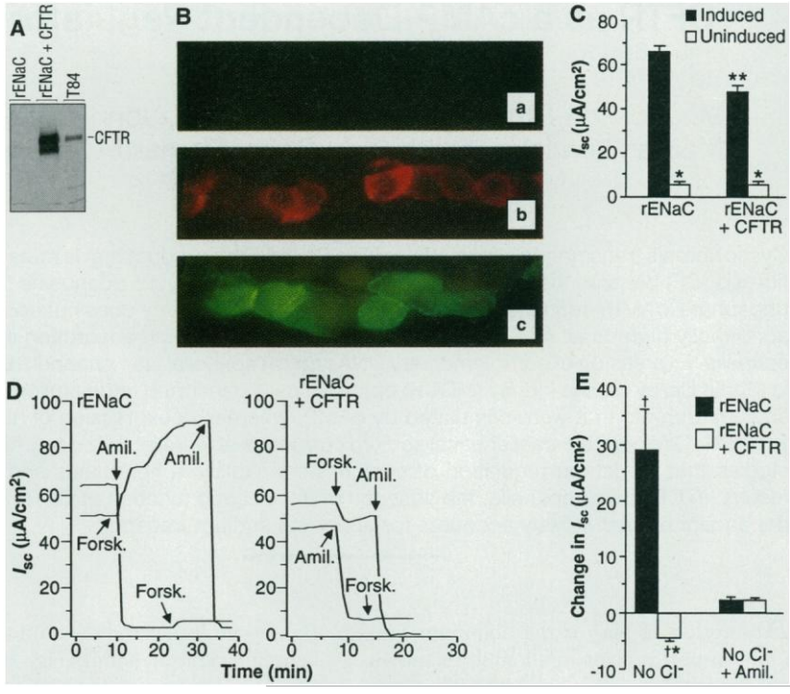

Fig. 2. Effect of human CFTR expression on MDCK Na^+ absorption. (**A**) CFTR protein in MDCK/rENaC cells before and after infection with Ad5-CB*CFTR* as shown by protein immunoblot analysis. CFTR protein in T84 cells is shown for comparison. (**B**) Immunocytochemistry of control cells (a) and MDCK/rENaC cells (b) stained for α-rENaC, and MDCK/rENaC cells (c) expressing adenoviral vector–transduced CFTR stained for CFTR 24 hours after infection. (**C**) Effect of CFTR expression on basal MDCK I_{sc} in Cl^--free solution. Cells denoted rENaC are MDCK/rENaC cell layers that were control-infected with *lacZ* or exposed to 10% glycerol only and induced as in Fig. 1 (n = 12) or not induced (n = 11). Cells denoted rENaC + CFTR are MDCK/rENaC cell layers that were infected with Ad5-CB*CFTR* (*15*) adenovirus containing human CFTR cDNA and induced as in Fig. 1 (n = 10) or not induced (n = 6). An asterisk denotes a significant difference between induced and uninduced currents (unpaired t analysis, $P < 0.05$); two asterisks denote a significant difference between the two induced currents (unpaired t analysis, $P < 0.05$). (**D**) Effect of raising intracellular cAMP on I_{sc} in induced MDCK/rENaC cells in bilateral Cl^--free solutions (left panel). The coexpression of human CFTR altered this effect (right panel). Data are from representative experiments with tissues that were preincubated in bilateral Cl^--free KBR for 45 min. Amiloride (Amil.) (mucosal, 10^{-4} M) and forskolin (Forsk.) (mucosal and serosal, 10^{-5} M) were added as indicated. (**E**) Forskolin-induced changes in Na^+ current. MDCK cells that were control-infected as in (C) and induced as in Fig. 1 (solid bars) were exposed to forskolin in Cl^--free solution without (n = 5) or with 10^{-4} M amiloride (n = 4); rENaC + CFTR cells (open bars) were similarly exposed to forskolin without (n = 14) or with 10^{-4} M amiloride (n = 6). A cross denotes a result significantly different from zero (paired t analysis, $P < 0.05$). An asterisk denotes a significant difference between the rENaC and rENaC + CFTR results (unpaired t analysis, $P < 0.05$).

these proteins in 3T3 fibroblasts (*19*) and used the whole-cell voltage clamp technique to control the Na^+ electrochemical potential as well as the activities of intracellular protons and Ca^{2+} (*20*). Fibroblasts were infected with a retrovirus expressing from a single tricistronic mRNA transcript the α, β, and γ rENaC cDNAs (*21*). Protein immunoblots and immunofluorescence studies revealed expression of α-, β-, and γ-rENaC in rENaC-transfected 3T3 fibroblasts (Fig. 3, A and C) but not parental cells (Fig. 3, B and D). Control 3T3 fibroblasts that were bathed and dialyzed with Na^+ aspartate (Cl^--free) solutions had small whole-cell currents that were not sensitive to amiloride (Fig. 4A, a and c). Fibroblasts that expressed rENaC exhibited induced inward basal currents that were inhibited by amiloride (Fig. 4A, b and c) and by benzamil and phenamil. In fibroblasts expressing rENaC alone, the permeant cAMP analog, cpt-cAMP, stimulated the inward Na^+ current (Fig. 4B, a). In contrast, when rENaC subunits were coexpressed with CFTR, cpt-cAMP inhibited the inward Na^+ current (Fig. 4B, b). All cpt-cAMP–induced changes in inward current, including the stimulated currents in rENaC cells and the inhibited currents in rENaC + CFTR cells, were abolished by amiloride pretreatment (Fig. 4B, c). Thus, as in MDCK cells, the presence of CFTR fundamentally alters regulation of rENaC-mediated Na^+ currents. These whole-cell data, obtained under conditions of controlled driving forces and no permeant anions, demonstrate that CFTR regulates the permeability of epithelial Na^+ channels.

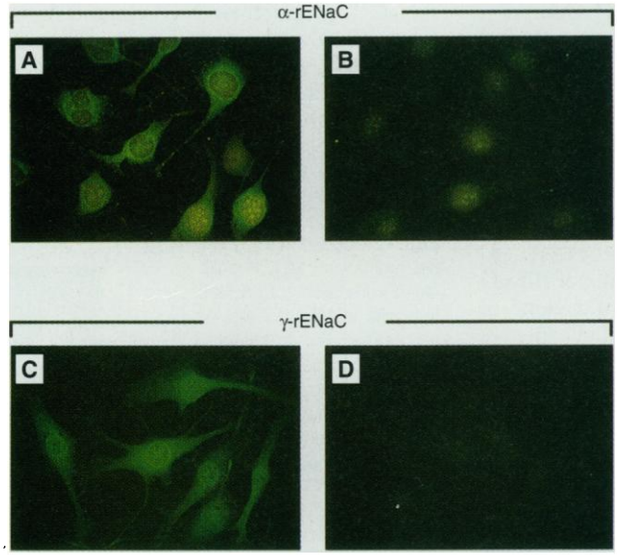

Fig. 3. Immunocytochemistry for α-rENaC and γ-rENaC expression in fibroblasts infected with a retrovirus containing a tricistronic vector for α, β, and γ cDNAs (**A** and **C**) and in parental (3T3) fibroblasts (**B** and **D**).

An earlier patch clamp study (*5*) and the recent observation that amounts of mRNA for Na^+ channel subunits are the same in CF and normal airways (*14*) are consistent with increased activity of Na^+ channels as the cause of abnormal Na^+ absorption in CF. We have identified a function for CFTR as a cAMP-dependent negative regulator of Na^+ channels that can account for raised Na^+ absorption in CF airways. As shown in Fig. 5, the combined functions of CFTR as a regulator of Na^+ channels and as a cAMP-regulated Cl^- channel suggest that CFTR is the "switch" that balances the rates of Na^+ absorption and Cl^- secretion to properly hydrate airway secretions in normal airway epithelia. CF airways lack

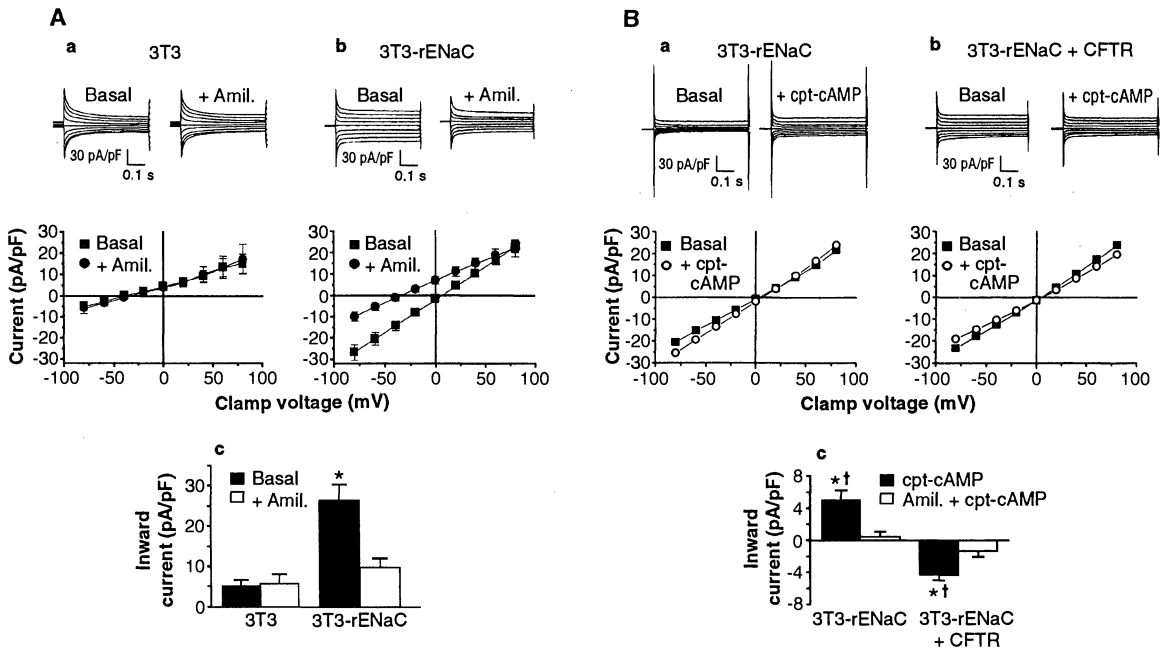

Fig. 4. (**A**) Basal and amiloride-sensitive whole-cell current in 3T3 cells expressing rENaC only (3T3-rENaC) versus controls (3T3). Whole-cell currents were measured in 3T3 cells (a) and 3T3-rENaC cells (b). The steady-state current recorded with Cl^--free bath and pipette solutions before the addition of amiloride (10^{-5} M) (Basal) and the current recorded after 2 to 4 min of amiloride (+ Amil.) are shown. Representative families of whole-cell current jumps in response to 0.45-s voltage pulses originating from 0 mV and covering ±80 mV in 20-mV increments are shown in the top portion of each panel, and mean current-voltage plots for 5 different 3T3 cells and 17 different 3T3-rENaC cells are shown in the lower portion. (c) Inward current recorded at −80 mV without and with 10^{-5} M amiloride. (**B**) cAMP-dependent modulation of rENaC-mediated whole-cell current without or with coexpressed CFTR. Whole-cell currents were measured in 3T3-rENaC cells (a) and 3T3-rENaC + CFTR cells (b) in Cl^--free bath and pipette solutions. After steady-state currents were recorded (Basal), cpt-cAMP was added to the bath (final concentration 5×10^{-4} M); the new steady-state current was recorded 5 to 10 min later (+ cpt-cAMP). Representative experiments are shown in the top portion of each panel, and mean current-voltage plots are shown in the lower portion ($n = 8$). (c) Induced inward current at −80 mV without and with 10^{-5} M amiloride. The change in 3T3-rENaC cells was stimulation ($n = 8$), whereas the change in 3T3-rENaC + CFTR cells was inhibition ($n = 8$). These changes represent a 29% stimulation of basal amiloride-sensitive current in 3T3-rENaC fibroblasts (16.9 ± 2.8 pA/pF, $n = 17$) and a 40% inhibition of basal amiloride-sensitive current in 3T3-rENaC + CFTR fibroblasts (10.7 ± 2.0 pA/pF, $n = 9$). Asterisks and crosses denote significant differences from zero and from amiloride pretreatment, respectively ($P < 0.05$).

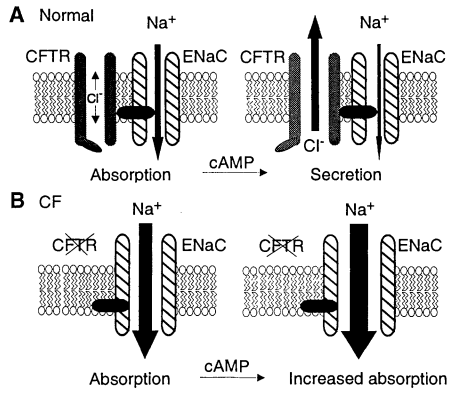

Fig. 5. Model of ENaC and CFTR functional interactions. (**A**) Conditions in normal airway epithelium. CFTR and ENaC are present in the apical cell membrane. These conditions were recreated in MDCK/rENaC + CFTR cells and in 3T3-rENaC + CFTR cells. In this model, cAMP positively regulates CFTR, which is proposed to exert a negative effect on ENaC. This interaction is depicted by the solid bar that partially occludes the ENaC pore, but no specific mechanism is implied. Possibilities include direct interaction of CFTR with ENaC or through other cAMP-dependent mechanisms (including cytoskeletal elements and membrane recycling) or other regulatory proteins (*22, 23*). (**B**) Conditions in CF airway epithelial cells, which lack functional CFTR in the apical membrane but express ENaC. Similar conditions were found in MDCK/rENaC cells (low endogenous CFTR) and 3T3-rENaC cells (no endogenous CFTR). The absence of negative regulation by CFTR leaves the stimulatory effect of cAMP on ENaC function unopposed.

CFTR and the absence of the switch results in increased Na^+ channel activity and Na^+ hyperabsorption. CFTR and ENaC may interact directly through cytoskeletal elements or regulatory proteins (*22*) or through soluble extracellular mediators released by CFTR (*23*).

The emerging concept of CFTR as a multifunctional protein (*23*) provides insights into the pathogenesis of CF lung disease, which has not been adequately explained solely by abnormal Cl^- channel function. Further investigations that focus on the modes of regulation of Na^+ channels by CFTR may identify novel therapeutic strategies to treat CF lung disease.

REFERENCES AND NOTES

1. R. C. Boucher, *Am. J. Respir. Crit. Care Med.* **150**, 271 (1994).
2. ———, M. J. Stutts, M. R. Knowles, L. Cantley, J. T. Gatzy, *J. Clin. Invest.* **78**, 1245 (1986).
3. N. J. Willumsen and R. C. Boucher, *Am. J. Physiol.* **261**, C319 (1991).
4. ———, *ibid.*, p. C332.
5. T. C. Chinet, J. M. Fullton, J. R. Yankaskas, R. C. Boucher, M. J. Stutts, *ibid.* **266**, C1061 (1994).
6. C. M. Canessa, J.-D. Horisberger, B. C. Rossier, *Nature* **361**, 467 (1993).
7. C. M. Canessa *et al.*, *ibid.* **367**, 463 (1994).
8. R. P. Hirt, O. Poulain-Godefroy, J. Billotte, J. Kraehenbuhl, N. Fasel, *Gene* **111**, 1827 (1992).
9. C. Canessa, in preparation.
10. W. O'Neal, T. Ecay, J. Katkin, W. Dubinsky, *Pediatr. Pulmonol.* (suppl. 10) (1994), p. 194. A clone of wild-type MDCK cells selected for high transepithelial resistance was transfected with separate cDNA constructs encoding for rat α-, β-, and γ-rENaCs and for neomycin resistance (neo^r). The studies reported here used G418-resistant clone 29.1 (*9*), designated MDCK/rENaC. MDCK/rENaC cells were induced in G418 (250 μg/ml), 10^{-6} M amiloride, 10^{-6} M dexamethasone, and 2 mM butyrate overnight. Noninduced control MDCK/rENaC cells were maintained in G418 only. Parent nontransfected MDCK cells were induced without G418.
11. Induced MDCK/rENaC cells were metabolically labeled with [^{35}S]methionine (*24*) and a microsomal fraction was immunoprecipitated with antibodies raised against α, β, or γ subunits of rENaC (*7, 25*). Immunoprecipitated proteins were separated on 10% resolving SDS–polyacrylamide gel electrophoresis (*26*) and assayed by Amplify (Amersham). Cells were grown on permeable collagen supports and short-circuit current (I_{sc}), which was measured as in (*18, 27*). The bathing solutions were based on the composition of Krebs-bicarbonate-Ringer (KBR); Cl^--free KBR was made by replacing all Cl^- salts with gluconate salts (*3, 28*).
12. B. R. Grubb, A. M. Paradiso, R. C. Boucher, *Am. J. Physiol.* **267**, C293 (1994).
13. G. Champigny *et al.*, *EMBO J.* **13**, 2177 (1994).
14. C. R. Talbot, L. Burch, R. C. Boucher, *FASEB J.* **9**, 304 (1995); L. H. Burch *et al.*, *Am. J. Physiol.*, in press.
15. B. R. Grubb *et al.*, *Nature* **371**, 802 (1994).
16. Protein immunoblot analysis of cell lysates of MDCK and T84 cells for human CFTR were performed as

described (19). Immunofluorescence of α-rENaC (7) used a polyclonal antibody against a glutathione-S-transferase fusion protein containing the first 76 amino acids of the NH_2-terminus (29) and CFTR protein-1468 (30), following the protocol of Grubb *et al.* (15). Cells on coated cover slips were fixed in acetone at 20°C for 10 min and incubated in primary antibodies for 90 min at room temperature followed by fluorescein isothiocyanate (FITC)– and Texas Red–conjugated secondary antibodies for 30 min. Parent MDCK cells were used as control. Similar results were obtained for the rENaC subunit.
17. H. H. Ussing, *Physiol. Rev.* **29**, 127 (1949).
18. C. U. Cotton, M. J. Stutts, M. R. Knowles, J. T. Gatzy, R. C. Boucher, *J. Clin. Invest.* **79**, 80 (1987).
19. M. J. Stutts *et al.*, *J. Biol. Chem.* **268**, 20653 (1993).
20. We studied 3T3 cells on the stage of an inverted microscope at 22°C by the techniques of Hamill *et al.* (31). Pipettes were filled with Cl^--free buffer that contained 100 mM Na aspartate, 2 mM $MgSO_4$, 2 mM Na_2ATP, and 5 mM *N*-tris(hydroxymethyl)-methyl-2-aminoethanesulfonic acid (TES) (pH 7.2). Cl^--free extracellular buffer contained 160 mM Na gluconate, 2 mM $MgSO_4$, 1 mM $CaSO_4$, and 5 mM TES (pH 7.2). [See (32) for other details.] Solutions containing amiloride (final concentration 10^{-5} M) and cpt-cAMP (5×10^{-4} M)/forskolin (1×10^{-5} M) were added by a 1:2 dilution of the extracellular bath.
21. Swiss 3T3 fibroblasts stably expressing the human CFTR gene (32) or an inactive interleukin-2 receptor (33) were infected with a retrovirus expression vector encoding the α-, β-, and γ-rENaC subunits. The three subunits were expressed from the viral long terminal repeat on a tricistronic mRNA in the order (5′ to 3′) α, β, γ. Internal ribosomal entry site sequences from encephalomyocarditis virus and poliovirus were included 5′ of the β and γ subunit sequences, respectively, to facilitate translation. Immediately 3′ to the γ subunit, an SV40 promoter was included to drive transcription of a puromycin-selectable marker. Fibroblasts were exposed to virus (10^2 CFU/ml) in polybrene (8 μg/ml) and were selected in puromycin (1 μg/ml). Resistant colonies were expanded and expression of α-, β-, and γ-rENaC subunits was determined by Northern (RNA) blot and protein immunoblot analyses. Immunocytochemistry was as described in Fig. 2.
22. D. A. Ausiello, J. L. Stow, H. F. Cantiello, J. B. de Almeida, D. J. Benos, *J. Biol. Chem.* **267**, 4759 (1992).
23. I. L. Reisin *et al.*, *ibid.* **269**, 20584 (1994); E. M. Schwiebert, T. Flotte, G. R. Cutting, W. B. Guggino, *Am. J. Physiol.* **266**, C1464 (1994).
24. S. Laferte and L. C. Loh, *Biochem. J.* **283**, 193 (1992).
25. R. M. Rios, C. Celati, S. M. Lohmann, M. Bornens, G. Keryer, *EMBO J.* **11**, 1723 (1992).
26. B. Sarkadi *et al.*, *J. Biol. Chem.* **267**, 2087 (1992).
27. N. J. Willumsen, C. W. Davis, R. C. Boucher, *Am. J. Physiol.* **256**, C1033 (1989).
28. B. R. Grubb, R. N. Vick, R. C. Boucher, *ibid.* **266**, C1478 (1994).
29. C. M. Canessa, A. Merillat, B. C. Rossier, *ibid.* **267**, C1682 (1994).
30. J. A. Cohn, O. Melhus, L. J. Page, K. L. Dittrich, S. R. Vigna, *Biochem. Biophys. Res. Commun.* **181**, 36 (1991).
31. O. P. Hamill, A. Marty, E. Neher, B. Sakmann, F. J. Sigworth, *Pfluegers Arch.* **391**, 85 (1981).
32. M. J. Stutts *et al.*, *J. Biol. Chem.* **269**, 8667 (1994).
33. J. C. Olsen *et al.*, *Hum. Gene Ther.* **3**, 253 (1992).
34. We thank P. Blonigen, H. Suchindran, U. S. Rao, and H. Ye for technical contributions and L. Brown for editorial assistance. Supported by NIH grants HL 34322, HL 42384, and CFF R026 and by Swiss National Foundation grant 31-33598.92.

23 February 1995; accepted 19 June 1995

Ultrasound-Mediated Transdermal Protein Delivery

Samir Mitragotri, Daniel Blankschtein,* Robert Langer*

Transdermal drug delivery offers a potential method of drug administration. However, its application has been limited to a few low molecular weight compounds because of the extremely low permeability of human skin. Low-frequency ultrasound was shown to increase the permeability of human skin to many drugs, including high molecular weight proteins, by several orders of magnitude, thus making transdermal administration of these molecules potentially feasible. It was possible to deliver and control therapeutic doses of proteins such as insulin, interferon γ, and erythropoeitin across human skin. Low-frequency ultrasound is thus a potential noninvasive substitute for traditional methods of drug delivery, such as injections.

Transdermal drug delivery (TDD) offers several advantages over traditional delivery methods such as injections and oral administration. Compared to oral delivery, TDD avoids gastrointestinal drug metabolism, reduces elimination by liver, and provides sustained release of drugs for up to 7 days (*1*). Compared to injections, TDD eliminates the associated pain and the possibility of infection. Theoretically, the transdermal route of drug administration could be advantageous in the delivery of many therapeutic proteins because (i) proteins are susceptible to gastrointestinal degradation and exhibit poor gastrointestinal uptake, (ii) proteins such as interferons are cleared rapidly from the blood (*2*) and need to be delivered at a sustained rate in order to be maintained at a high blood concentration, and (iii) transdermal devices are easier to use than injections (*1*).

Despite these advantages, few drugs and no proteins or peptides are currently administered transdermally for clinical applications, because of the low skin permeability to drugs. This low permeability is attributed to the stratum corneum (SC), the outermost skin layer that consists of flat, dead cells filled with keratin fibers (keratinocytes) surrounded by lipid bilayers. The highly ordered structure of the lipid bilayers confers an impermeable character to the SC (*3*). Several methods, which include chemical enhancers (*4*) and electricity (*5*, *6*), have been proposed to enhance transdermal drug transport, but their efficacy has been limited by the large protein size and relatively low electric charge on the proteins.

Application of ultrasound has been attempted to enhance transdermal transport of a few low molecular weight (<500) drugs across human skin (*7*–*10*) as well as proteins such as insulin across animal skin (*11*), a phenomenon referred to as sonophoresis. Although numerous studies of sonophoresis have been performed (*7*–*11*) measurable enhancement has been reported in only a few cases (*8*, *11*). We have shown (*12*) that application of ultrasound at therapeutic frequencies (1 MHz) induces growth and oscillations of air pockets present in the keratinocytes of the SC (a phenomenon known as cavitation). These oscillations disorganize the SC lipid bilayers, thereby enhancing transdermal transport. However, application of therapeutic ultrasound does not induce transdermal transport of high molecular weight proteins. Because cavitational effects are inversely proportional to ultrasound frequency (*13*), we hypothesized that application of ultrasound at frequencies lower than that corresponding to therapeutic ultrasound may induce sufficient bilayer disorganization, so that proteins may be able to diffuse across the skin. We now report that low-frequency ultrasound can induce significant transdermal transport of proteins, including insulin (molecular weight, ~6000), interferon γ (IFN-γ) (~17,000), and erythropoeitin (~48,000).

The passive skin permeability to high molecular weight proteins, including those mentioned above, is essentially zero (below our detection limit). To assess whether application of ultrasound enhances transdermal protein flux, we measured the skin permeability to these proteins in the presence of ultrasound in vitro across human cadaver epidermis (*14*) in a Franz diffusion cell (*15*). In separate experiments, the donor compartment of the diffusion cell was filled with a solution of insulin (100 U/ml), IFN-γ (2500 U/ml), or erythropoeitin (400 U/ml). Ultrasound (20 KHz, 100-ms pulses applied every second) was applied at intensities in the range of 12.5 to 225 mW/cm^2 (*16*) for 4 hours by means of an ultrasound transducer that was immersed in the donor solution. The transducer (area, ~1 cm^2) was oriented perpendicular to, and placed at a distance of 1 cm from, the skin. The concentration of

Department of Chemical Engineering, Massachusetts Institute of Technology, Cambridge, MA 02139, USA.

*To whom correspondence should be addressed.